












RESEARCH LETTER

A Pellino-2 variant is associated with constitutive NLRP3 inflammasome activation in a family with ocular pterygium–digital keloid dysplasia

Ileana Cristea^{1,2} , Hugo Abarca³ , Anne E. Christensen Mellgren^{1,2} , Milana Trubnykova^{3,4} ,
 Roya Mehrasa^{1,5} , Dorien J. M. Peters⁶ , Gunnar Houge⁵ , Raoul C. M. Hennekam^{7,8} ,
 Eyvind Rødahl^{1,2} , Ove Bruland⁵  and Cecilie Bredrup^{1,2,5} 

- 1 Department of Clinical Medicine, University of Bergen, Norway
- 2 Department of Ophthalmology, Haukeland University Hospital, Bergen, Norway
- 3 Servicio de Genética & Errores Innatos del Metabolismo, Instituto Nacional de Salud del Niño-Breña, Lima, Peru
- 4 Facultad de Ciencias de la Salud, Universidad Peruana de Ciencias Aplicadas, Lima, Peru
- 5 Department of Medical Genetics, Haukeland University Hospital, Bergen, Norway
- 6 Department of Human Genetics, Leiden University Medical Center, The Netherlands
- 7 Department of Pediatrics, Emma Children's Hospital, Amsterdam, The Netherlands
- 8 Department of Clinical Genetics, Academic Medical Center, University of Amsterdam, The Netherlands

Correspondence

C. Bredrup, Department of Ophthalmology, Haukeland University Hospital, Jonas Lies vei 72B, Bergen 5021, Norway
 Tel: (+47) 55974171
 E-mail: cecilie.bredrup@uib.no

(Received 10 November 2022, revised 16 January 2023, accepted 26 January 2023, available online 24 February 2023)

doi:10.1002/1873-3468.14597

Edited by Wilfried Ellmeier

Ocular pterygium–digital keloid dysplasia (OPDKD) is a rare hereditary disease characterized by corneal ingrowth of vascularized conjunctival tissue early in life. Later, patients develop keloids on fingers and toes but are otherwise healthy. In a recently described family with OPDKD, we report the presence of a *de novo* c.770C > T, p.(Thr257Ile) variant in *PELI2* in the affected individual. *PELI2* encodes for the E3 ubiquitin ligase Pellino-2. In transgenic U87MG cells overexpressing Pellino-2 with the p.(Thr257Ile) amino acid substitution, constitutive activation of the NLRP3 inflammasome was observed. However, the Thr257Ile variant did not affect Pellino-2 intracellular localization, its binding to known interaction partners, nor its stability. Our findings indicate that constitutive autoactivation of the NLRP3 inflammasome contributes to the development of *PELI2*-associated OPDKD.

Keywords: corneal vascularization; keloids; NLRP3 inflammasome; OPDKD; *PELI2*; pterygium

Abbreviations

Asn, asparagine amino acid; ATP, adenosine triphosphate; CHX, cycloheximide; DVL-2, disheveled segment polarity protein 2; ELISA, enzyme-linked immunosorbent assay; FHA, forkhead-associated domain; FSCN2, fascin-2; GJB2, gap junction beta 2; HEK293 cells, human embryonic kidney cells; IL-1 β , interleukin 1 beta; Ile, isoleucine amino acid; IRAK-1, interleukin 1 receptor-associated kinase 1; IRAK-4, interleukin 1 receptor-associated kinase 4; IRS1, insulin receptor substrate 1; K⁺, potassium ions; LPS, lipopolysaccharides; LRT, log ratio test; MAP3K7, mitogen-activated protein kinase 7; MT, mutation taster; NDUFAF6, NADH ubiquinone oxidoreductase complex assembly factor 6; NEK7, NIMA-related kinase 7; NEK9, NIMA-related kinase 9; NLRP3, NLR family pyrin domain containing 3; OMIM, Online Mendelian Inheritance in Man; OPDKD, ocular pterygium-digital keloids dysplasia; PAX6, paired box protein 6; PDGFR β , platelet-derived growth factor receptor beta; p_i, isoelectric point; PP, PhyloP; PP2, PolyPhen2; ROBO-1, roundabout homolog 1; SCL44A1, choline transporter-like protein 1; TAB2, TGF- β activated kinase 1 (MAP3K7)-binding protein 2; TAK1, transforming growth factor β -activated kinase 1; TBR1, T-box brain protein 1; TLR, toll-like receptor; Thr, threonine amino acid; TRAF6, TNF receptor-associated factor 6; TRAF7, TNF receptor-associated factor 7; Tyr, tyrosine amino acid; WES, whole exome sequencing; WT, wild-type.

Early onset corneal vascularization can be seen in a range of hereditary conditions such as *PAX6*-associated keratopathy [1], dyskeratosis congenita (*DKC1*, *TERC*, *TERT*, *NOPI0*, *NHP2*, *TINF2*, *C16orf57*, *TCABI*) [2] and Warburg-Cinotti syndrome (*DDR2*) [3]. In addition, it is also a key feature of ocular pterygium–digital keloid dysplasia (OPDKD). This rare autosomal dominant hereditary disease is characterized by corneal vascularization leading to visual impairment early in life. Most patients also develop keloids on fingers and toes but are otherwise healthy [4–6]. We recently described two families presenting with OPDKD [4,6]. Genetic analysis of one of them identified a variant in *PDGFRB* associated with the condition [4].

For this study, we included the second family consisting of an individual with OPDKD and his healthy family members. Exome sequencing did not reveal any unusual variants in *PDGFRB*. Instead, by trio exome sequencing, a *de novo* variant in the *PELI2* gene (MIM#614798) was found, encoding the E3 ubiquitin ligase Pellino-2. In U87MG cells overexpressing the c.770C > T, p.(Thr257Ile) *PELI2* variant, we observed the constitutive activation of the NLRP3 inflammasome and increased levels of secreted IL-1 β . This suggests that OPDKD might be associated with increased inflammation caused by a variant in *PELI2*.

Materials and methods

Patient enrollment and ethical approval

In 2014, Abarca *et al.* [6] reported a patient with OPDKD. Conjunctival ingrowth of the cornea was observed from childhood, and he was given the diagnosis of pterygium at the age of 7 years. After undergoing surgery 2 years later, rapid recurrence of corneal vascularization was seen. Despite treatment, the ocular changes progressed, leading to severely reduced vision [6]. The keloids on his toes and fingers, together with the corneal symptoms, were similar to changes reported by Haugen and Bertelsen [7] and the condition was named OPDKD.

This study was approved by the Regional Committee for Medical and Health Research Ethics, Western Norway (IRB.no. 00001872, project number 2014/59). Informed written consent was obtained from the affected individual and healthy controls prior to the collection of blood samples and skin biopsies. The study thus adhered to the Tenets of the Declaration of Helsinki.

Trio exome sequencing

DNA extracted from peripheral blood from the affected individual and his parents was subjected to whole exome sequencing (WES) at HUDSONALPHA (HudsonAlpha Genomic

Services Laboratory, Huntsville, AL, USA) using Nimble-Gen v3 exome capture and sequenced on Illumina HiSeq with 2 × 100 bp reads and an estimated median coverage of 75×. Illumina BCL files were converted to fastq files by HUDSONALPHA. Trimming (TRIMMOMATIC-0.33), alignment (BWA-0.6.2) to GRCh37.1, realignment, and variant calling (PICARD-tools-1.129 and GENOMEANALYSISSTK-2.7.4) [8] were performed by us following the Broad recommended best practice guidelines [9]. VCFTOOLS v.0.1.9 was used for filtering variants [10], and ANNOVAR [11] was used for annotation.

Generation of transduced cell lines

Transduced HEK293 and U87MG cells, stably overexpressing wild-type (WT) *PELI2* (NM_021255.3) or the c.770C > T, p.(Thr257Ile) variant with a C-terminal HA tag, were generated by transduction with the constructs described below [12]. Virus production was performed by transfecting PHOENIX-AMPHO packaging cells (CRL-3213; ATCC, Manassas, VA, USA) as described previously [13]. Two days after transfection, the medium was harvested and the immortalized cell lines HEK293 (CRL-1573TM; ATCC) and U87MG (HTB-14TM; ATCC) were transduced following standard protocols [14]. The cells were grown in DMEM containing 10% fetal bovine serum. Two days postinfection, stably transduced cells were selected by adding 1 $\mu\text{g}\cdot\text{mL}^{-1}$ puromycin (cat# ant-pr-1; InvivoGen, San Diego, CA, USA) to the culture medium, and kept thereafter in the selection medium for additional 14 days.

Quantification of secreted IL-1 β upon NLRP3 inflammasome activation

Nontransduced and transduced U87MG cells were seeded in tissue-culture 96-well plates (#9018; Corning Costar, Corning, NY, USA) at a density of 75 000 cells per well in 300 μL of U87MG culture medium.

On the day of the assay, cells were primed with 100 $\text{ng}\cdot\text{mL}^{-1}$ LPS (*E. coli* O111:B4, #LPS25; Sigma-Aldrich, St. Louis, MO, USA) for 3 h, to upregulate genes necessary for NLRP3 inflammasome activation, and activated with 5 mM ATP (#R0441; Thermo Fischer Scientific, Waltham, MA, USA) for 30 min. After incubation, supernatants were collected and assayed for IL-1 β release using a human IL-1 β ELISA kit (#88-7261-88; Thermo Fischer Scientific) according to the manufacturer's protocol, as previously described [12].

Cell viability assay

Cell proliferation/viability following NLRP3 inflammasome activation in transduced U87MG cells was assessed by WST-1 assay. Twenty-four hours after inflammasome activation, the WST-1 reagent (#5015944001; Roche Diagnostics, Mannheim, Germany) was added into the wells at a

1 : 10 dilution and incubated for 4 h at 37 °C. The optical density (OD) was measured at wavelength 440 nm with correction at 650 nm, using a Synergy™ HT microplate reader (Agilent, Santa Clara, CA, USA).

Cell culture

Primary cell culture of human fibroblasts was established, as previously described [15]. These and the immortalized cell lines HEK293 (ATCC CRL-1573™) and U87MG (ATCC HTB-14™) were cultured under standard conditions [16].

Immunofluorescence

Primary skin fibroblasts were seeded on 12-mm glass cover-slips, in 24-well plates. The staining procedure was performed as previously described [16]. Briefly, the cells were fixed with 3% PFA in either PBS pH 7.4 or 0.1 M phosphate buffer pH 7.2 for 30 min, followed by permeabilization and blocking. Primary antibody staining against endogenous Pellino-2 (1 : 50, HPA053182; Sigma-Aldrich) was followed by secondary antibody incubation and washing before imaging was performed using a Leica SP8 confocal microscope (Deerfield, IL, USA).

Expression vectors

A TRAF7-HA (vector ID: VB160907-1025yut) encoding plasmid was purchased from VectorBuilder Biosciences (Guangzhou, China) Inc. The HA tag was replaced with a myc tag (primer pairs in Table S2).

The C-terminal HA-tagged wild-type Pellino-2 construct has been described previously [12]. The construct carrying the c.770C > T variant was generated using the Quik-Change II site-directed mutagenesis kit (Agilent).

Transient transfection, cell lysis, and co-immunoprecipitation

Nontransduced and transduced HEK293 cells were seeded in 10-cm dishes and cultured until 70–80 % confluency. For TRAF7 detection, the HEK293 cells were transiently transfected as previously described [16], with the TRAF7-myc expression vector, described above.

For detection of Pellino-2 interaction partners, the cells were lysed in cold lysis buffer and inputs were aliquoted, before the cell supernatants were incubated with anti-HA magnetic beads (#88837; Thermo Fischer Scientific) for 30 min at room temperature, according to manufacturer's instructions. The beads were washed 4 × 3 min with washing buffer, before boiling the samples at 98 °C for 10 min. The exact composition of the lysis buffer and the washing buffer for each individual interaction partner studied can be found in Table S3.

Immunoblot analysis

Protein detection was performed as previously described [16]. Briefly, co-immunoprecipitated samples were subjected to immunoblot analysis with primary antibodies against DVL-2 (#3216; Cell Signaling Technologies, Danvers, MA, USA), NEK9 (ab138488; Abcam, Cambridge, UK), ROBO-1 (ab7279; Abcam), cyclin F (sc-952; Santa Cruz Biotechnology, Dallas, TX, USA), IRAK-1 (#4504; Cell Signaling Technologies), IRAK-4 (#4363; Cell Signaling Technologies), TRAF6 (#8028; Cell Signaling Technologies), TAK1 (#4505; Cell Signaling Technologies), as well as the HA tag (71-5500; Thermo Fischer Scientific), followed by incubation with HRP-linked anti-rabbit IgG secondary antibody (#7074; Cell Signaling Technologies). Chemiluminescence was detected using the ChemiDoc Touch Imaging System (Biorad, Hercules, CA, USA).

Cycloheximide chase assay

Transduced HEK293 cells were seeded in 6-well dishes at 5×10^5 cells per well. At 70–80% confluency, the cells were treated with $10 \mu\text{g}\cdot\text{mL}^{-1}$ cycloheximide (#C4859-1ML; Sigma-Aldrich) for 4 and 8 h, followed by cell lysis and immunoblotting.

Statistical analysis

Two-way ANOVA, followed by the Tukey's multiple comparisons test, was performed for statistical analysis. All results have been replicated in at least three independent experiments.

Results

Genetic analysis

Trio exome sequencing was performed in the index patient and parents, and filtration was performed looking for homozygous, compound heterozygous, or *de novo* mutations that could be associated with the disease. We filtered common variants (allele frequency ≥ 0.01) using an in-house database, ESP6500, 1 kG, and dbSNP137. No genes with compound or homozygous variants could be associated with the phenotype of the index. Next, we isolated all the *de novo* variants and filtered those against the variants of the healthy sister. This left us with six *de novo* variants present in *TBRI*, *NDUFAF6*, *SCL44A1*, *GJB2*, *FSCN2*, and *PELI2* (Table 1). No unusual variants were seen in the coding region of *PDGFRB*.

Apart from *PELI2*, all these genes were already associated with a human disorder with phenotypes not overlapping that of OPDKD (Table 1). In addition,

Table 1. Novel gene variants with pathogenic potential. Following trio exome sequencing of the OPDKD family and filtering of common variants, six different pathogenic variants were identified, of which only two had been previously reported. AD, autosomal dominant; AR, autosomal recessive; DD, digenic dominant; het, heterozygous mutation; SNV, single nucleotide variant; X, stop codon.

Chr	Gene	Exon	Base change	Previously reported (database)	GT	Exonic function	Amino acid change	Encoded protein	Protein function	Associated genetic diseases
2	TBR1 (NM_006593)	6	c.T1240A	No	Het	Nonsynonymous SNV	p.Ser414Thr	T-box brain protein 1	Neuronal transcription factor, critical for normal brain development [36]	Sporadic autism and intellectual disability (OMIM #606053; AD)
8	NDUFAF6 (NM_152416)	4	c.G466A	Yes (gnomAD)	Het	Nonsynonymous SNV	p.Val156Ile	NADH:ubiquinone oxidoreductase complex assembly factor 6 (NDUFAF6)	Mitochondrial complex I deficiency, nuclear type 17 (OMIM #618239; AR), or Fanconi renotubular syndrome 5 (OMIM #618913; AR)	Mitochondrial complex I deficiency, nuclear type 17 (OMIM #618239; AR), or Fanconi renotubular syndrome 5 (OMIM #618913; AR)
9	SLC44A1 (NM_080546)	3	c.G181T	No	Het	Stop gain SNV	p.Gly61X	Choline transporter-like protein 1	Choline transport	Muscular, hepatic, and neurodegenerative diseases (OMIM #618868; AR) [37]
13	GJB2 (NM_004004)	2	c.T500G	No	Het	Nonsynonymous SNV	p.Val167Gly	Gap junction beta-2 protein	Structural component of gap junctions	Deafness digenic GJB2/GJB3 (OMIM #220290; AR, DD) Deafness autosomal recessive 1A (OMIM #220290; AR, DD) Deafness digenic GJB2/GJB6 (OMIM #220290; AR, DD)
14	PELI2 (NM_021255)	6	c.C770T	No	Het	Nonsynonymous SNV	p.Thr257Ile	Pellino-2	E3 ubiquitin ligase	Retinitis pigmentosa (OMIM #607921; AD/AR)
17	FSCN2 (NM_001077182)	1	c.G138T	Yes (gnomAD)	Het	Nonsynonymous SNV	p.Trp46Cys	Fascin-2	Actin bundling protein	

the identified variants had less predicted impact on protein structure (Table S1). The NM:021255:c.770C > T, p.(Thr257Ile) *PELI2* variant could not be found in the ClinVar, HGMD, or gnomAD databases of clinical, published, or population variants, respectively. Furthermore, it was predicted to be damaged by five different software programs: PhyloP, SIFT, PolyPhen2 (PP2), Log Ratio Test (LRT), and MutationTaster (MT). The CADD score was 26.0 (< 1% frequency type of variant, suggestive of pathogenicity). In the AlphaFold protein structure database, Thr257 occupies a highly conserved position in the protein (pLDDT score 97.95) with predicted interactions with Gly260, Leu261, and Asp242. Exchange from a polar threonine to a nonpolar isoleucine will probably disrupt at least some of these interactions. In addition, Pellino-2 is known to interact with TAK1 [16–18]. Mutations in *MAP3K7*, encoding TAK1, and its associated binding protein *TAB2* have been linked to keloid scar formation [19], leading us to conclude that *PELI2* was the most likely gene associated with the OPDKD phenotype in our patient.

Pellino-2 OPDKD substitution hyperactivates the NLRP3 inflammasome

Pellino-2 has been shown to facilitate LPS-induced NLRP3 inflammasome activation and production of IL-1 β [12,20]. Therefore, we wanted to investigate whether the OPDKD *PELI2* variant affected the protein's ability to participate in NLRP3 inflammasome activation. It has been shown that LPS and ATP administration induce NLRP3 inflammasome assembly in U87MG cells [21]. After transduction of U87MG cells with WT or Thr257Ile Pellino-2, baseline levels of IL-1 β secretion in nonactivated cells (NT) were statistically increased in the latter. This indicated that there is a constitutive activation of the NLRP3 inflammasome in cells transduced with the Thr257Ile variant (Fig. 1A). In line with this, after stimulation with LPS and ATP to activate the NLRP3 inflammasome, U87MG cells overexpressing the Thr257Ile Pellino-2 substitution showed significantly higher levels of secreted IL-1 β than cells transduced with the WT variant (Fig. 1A). Cell viability was not affected by LPS and ATP treatment (Fig. 1B). This suggested that the Thr257Ile variant induces NLRP3 inflammasome hyperactivation.

Pellino-2 OPDKD substitution does not affect intracellular Pellino-2 localization

Recently, the intracellular localization of Pellino-2 has been studied, in both immune and nonimmune cells

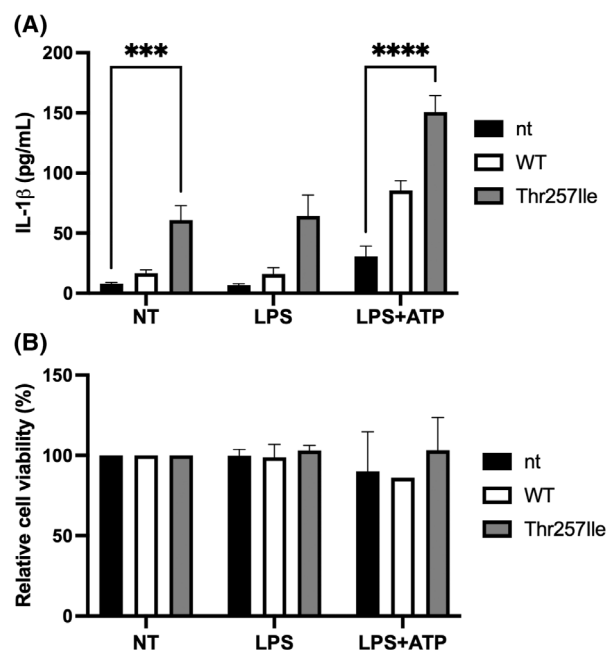


Fig. 1. Pellino-2 Thr257Ile variant leads to constitutive NLRP3 inflammasome activation. (A) Nontransduced (nt) and transduced U87MG cells overexpressing wild-type (WT) or the Pellino-2 Thr257Ile substitution with a C-terminal HA tag were left untreated (NT) or primed with LPS (100 ng·mL⁻¹ for 3 h) and activated with ATP (5 mM for 30 min), to induce NLRP3 inflammasome activation. Supernatants were harvested and the measurement of secreted IL-1 β was performed by ELISA. Data are shown as mean \pm SEM of three biological replicates, each with two technical replicates. Statistical analysis was performed using two-way ANOVA, followed by Tukey's test. *** P < 0.001, **** P < 0.0001. (B) The viability of the cells was measured 24 h after NLRP3 inflammasome activation, using the WST-1 assay. The WST-1 reagent was added in 1 : 10 dilution to the cells and incubated for 4 h at 37 °C. Data are shown as mean \pm SEM of three biological replicates.

[12,16]. Pellino-2 seems to relocate intracellularly upon efflux of K⁺ ions: in immune cells, Pellino-2 relocates to the site of the NLRP3 inflammasome activation, following K⁺ efflux [12]. In nonimmune cells, K⁺ efflux leads to the nuclear relocation of Pellino-2 [16].

We therefore performed immunofluorescence analysis of fibroblasts carrying the Thr257Ile Pellino-2 substitution, as well as age- and sex-matched controls, using K⁺-containing and K⁺-free fixation buffers (Fig. 2). Both cell lines displayed a similar pattern. Thus, in K⁺-containing PBS fixation buffer, WT, and Thr257Ile Pellino-2 were predominantly cytoplasmic (Fig. 2A). However, when K⁺-free PB fixation buffer was used, both WT and Thr257Ile Pellino-2 were predominantly nuclear (Fig. 2B).

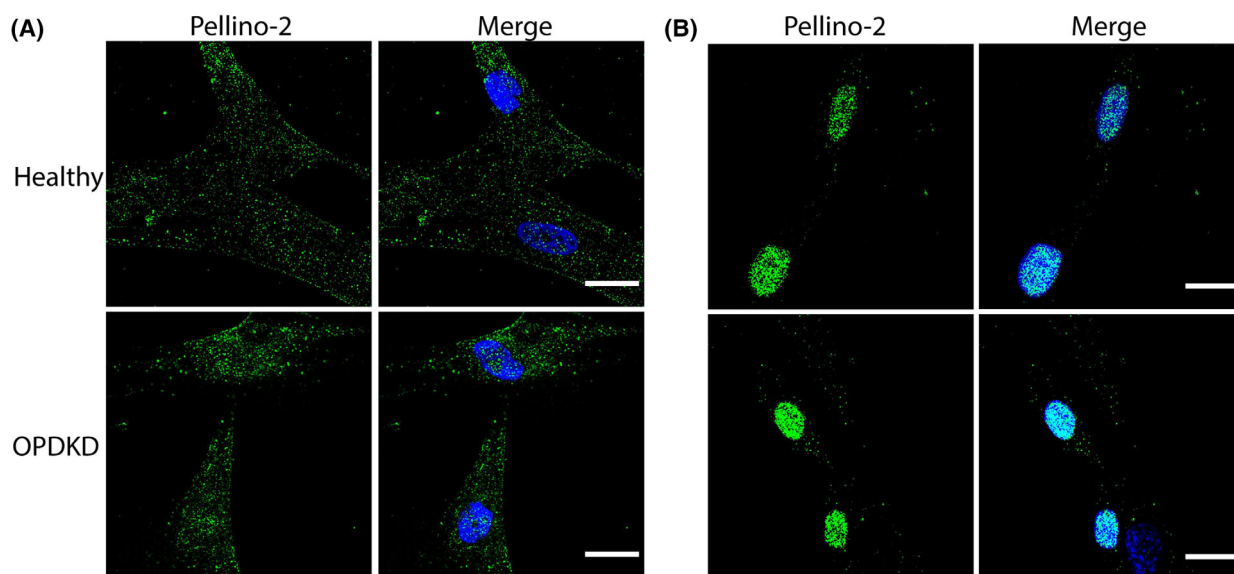


Fig. 2. Endogenous Pellino-2 changes localization depending on the fixation buffer. Immunofluorescence was performed in human primary fibroblasts from an age- and sex-matched healthy volunteer and the OPDKD patient, to detect endogenous Pellino-2. Fixation was performed with 3% PFA in (A) PBS pH 7.4 or (B) 0.1 M phosphate buffer (PB) pH 7.2. The fluorescent images show the endogenous protein (Pellino-2) and nuclei (DAPI). Scale bar: 20 μ m.

Pellino-2 OPDKD substitution does not affect the binding of Pellino-2 to known interaction partners

We have recently shown that Pellino-2 interacts with several proteins involved in various intracellular pathways and with different intracellular localizations. In addition to the classical toll-like receptor (TLR) pathway proteins, such as IRAK-1, TAK1, and TRAF6, Pellino-2 also binds to ROBO-1, NEK9, DVL-2, cyclin F, and TRAF7, as well as IRS-1 [16]. We therefore investigated if the Thr257Ile Pellino-2 substitution influences the binding of Pellino-2 to its interaction partners.

We performed co-immunoprecipitation with non-transduced HEK293 cells and transduced HEK293 cells (WT or Thr257Ile). Analysis of the inputs across experiments indicated that the endogenous levels of the interaction partners were not altered by the overexpression of either WT or Thr257Ile Pellino-2 (Fig. 3, left-hand side of the panel, labeled 'Inputs').

In addition, the Thr257Ile Pellino-2 substitution did not alter the binding between Pellino-2 and its interaction partners (Fig. 3). We were unable to study the interaction of Pellino-2 and IRS-1, due to low endogenous levels of the IRS-1 protein.

Although previous conflicting evidence suggests that Pellino-2 may be an interaction partner of the interleukin receptor-associated kinase IRAK-4 [22], we found

that neither WT nor Thr257Ile Pellino-2 bind to IRAK-4 (Fig. 3).

It should, however, be noted that under milder washing conditions, some interaction partners of Pellino-2 (DVL-2 and IRAK-1 but not TAK1, TRAF6, ROBO-1, NEK9, cyclin F, and TRAF7) consistently seemed to show less binding to the Thr257Ile *PELI2* variant (Fig. S1).

Pellino-2 OPDKD substitution does not affect Pellino-2 stability

We finally investigated the protein stability and turnover of Thr257Ile Pellino-2 compared with the WT in transduced HEK293 cells using a cycloheximide (CHX) chase assay. When protein synthesis was inhibited, there was no statistically significant difference in the turnover rates of the two proteins (Fig. 4).

Discussion

OPDKD is a rare hereditary condition, described only in a handful of families [4–7]. Previously, it has been associated with a temperature-sensitive mutation in *PDGFRB*. In this work, we identified a *de novo* variant in *PELI2*, c.770C > T, p.(Thr257Ile), in a patient with OPDKD. Bioinformatic analysis led us to conclude that the *PELI2* substitution was the most likely

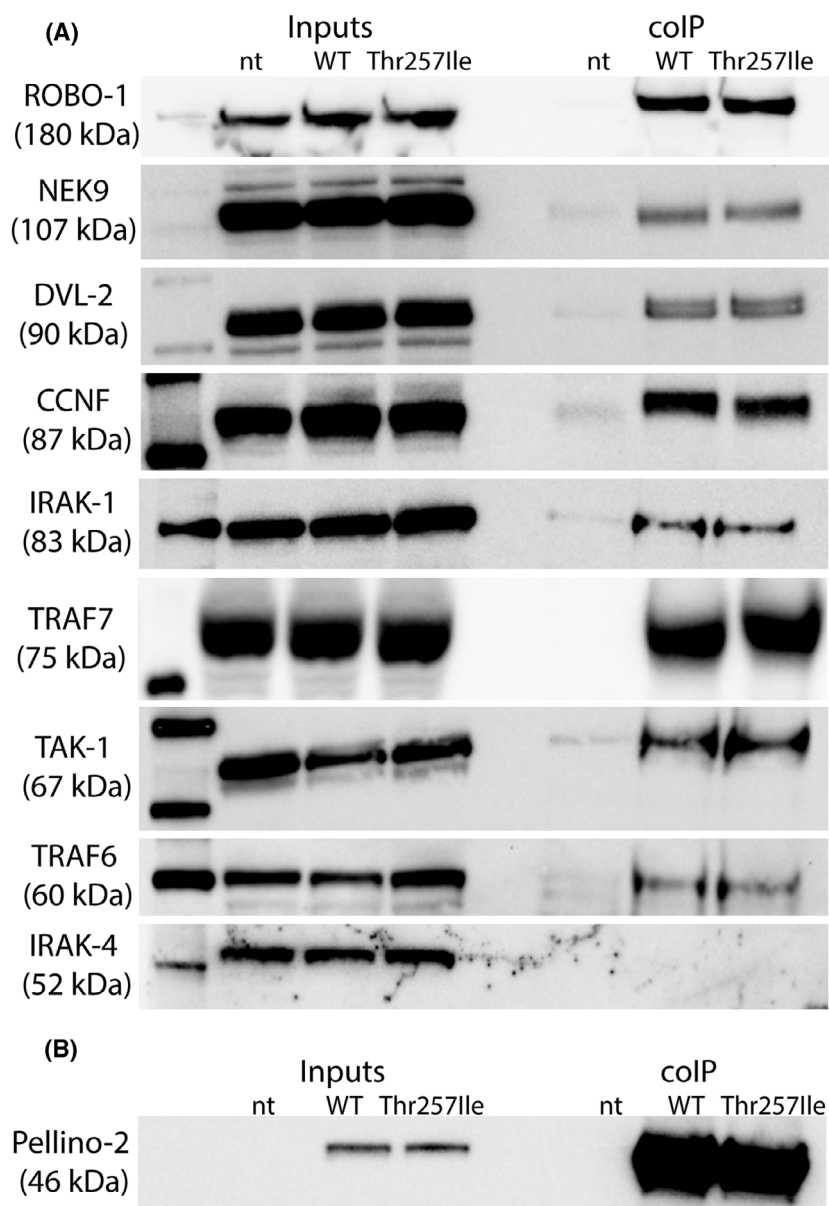


Fig. 3. Binding of Pellino-2 to its interaction partners is not affected by the *PELI2* OPDKD variant. (A) Nontransduced and transduced HEK293 cells stably overexpressing wild-type (WT) or the Pellino-2 Thr257Ile substitution with a C-terminal HA tag were co-immunoprecipitated using magnetic HA beads. Immunoblotting of known interaction partners of Pellino-2 was performed: ROBO-1, NEK9, DVL-2, cyclin F, IRAK-1, TAK1, TRAF6 and IRAK-4. For TRAF7 detection, nt, WT, and Thr257Ile HEK293 cells were transiently transfected with C-terminal myc-tagged TRAF7. Immunoblotting and myc detection following co-immunoprecipitation with magnetic HA beads was performed. (B) Immunoblotting and HA detection of stably overexpressed Pellino-2.

identified variant associated with OPDKD in the patient. The substitution leads to increased NLRP3 inflammasome activation, suggesting this could contribute to the observed corneal vascularization and keloid formation.

Pellino-2 is an E3 ubiquitin ligase in the TLR pathway. Following TLR activation, the level of pro-inflammatory cytokines is upregulated, alongside

elements of the NLRP3 inflammasome. In this work, we show that the Thr257Ile Pellino-2 substitution leads to constitutive activation of the NLRP3 inflammasome and increased secretion of IL-1 β in a transduced cell model (Fig. 1A).

Activation of the NLRP3 inflammasome has been observed in several disorders affecting the human

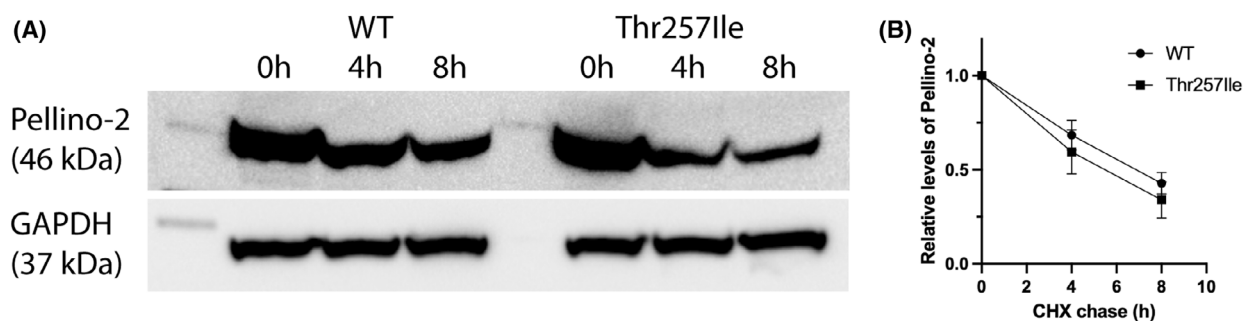


Fig. 4. Stability of Pellino-2 is not affected by the *PELI2* OPDKD variant. (A) HEK293 cells stably overexpressing wild-type (WT) or Pellino-2 with the Thr257Ile substitution were treated with $10 \mu\text{g}\cdot\text{mL}^{-1}$ cycloheximide (CHX). At the indicated time points, cell lysates were prepared, and immunoblotting analysis was performed against the HA tag of Pellino-2 and the internal control GAPDH. (B) The Pellino-2 band intensity was normalized to GAPDH and then normalized to the $t = 0$ h controls. Data are shown as mean \pm SEM in six different experiments ($n = 6$).

cornea. A gain-of-function variant in *NLRP3* leads to keratitis fugax hereditaria [23], with inflammatory attacks affecting the ocular surface. Additionally, persistent activation of the NLRP3 inflammasome has been found in both pterygium and keloids [24–28].

Pterygium is thought to be caused by focal limbal stem cell deficiency either by damage of the limbal stem cells or to the niche they reside in. The corneal vascularization in OPDKD resembles extensive pterygium formation, therefore damage of limbal stem cells due to chronic inflammation caused by constitutive NLRP3 inflammasome activation could be an initiating event in OPDKD [29,30].

The *PELI2* variant results in an amino acid substitution of a highly conserved amino acid residue, Thr257, in the N-terminal forkhead-associated (FHA) domain of the Pellino-2 protein. The N-terminal FHA domain has been shown to be the binding site for the ubiquitination substrates of Pellino-2 [31]. Several Pellino-2 binding partners are known to be involved in inflammasome activation. IRAK-1 and TAK1 have been proposed to suppress NLRP3 inflammasome activation [20,32]. By contrast, NEK7, a substrate of NEK9, has been shown to mediate inflammasome activation upstream of the NLRP3 inflammasome [33] and downstream of the K^+ efflux [34]. IRS-1, the first intracellular mediator of insulin signaling and one of the interaction partners of Pellino-2, has been shown to be downregulated by NLRP3 signaling and secreted IL-1 β [35]. We did not observe any statistically significant differences between the binding of WT and Thr257Ile Pellino-2 to ROBO-1, NEK9, DVL-2, cyclin F, TRAF7, IRAK-1, TAK1, and TRAF6 (Fig. 3) [16].

Pellino-2 has previously been shown to interact directly with the NLRP3 inflammasome [20]. Such a direct effect on the NLRP3 inflammasome provided by

the Thr257Ile amino acid substitution could theoretically explain the increased activation of the NLRP3 inflammasome.

In summary, we report a novel variant in the *PELI2* gene, c.770C > T, p.(Thr257Ile), in a patient with OPDKD. In functional studies, we show that the Thr257Ile substitution leads to a constitutive activation of the NLRP3 inflammasome. No effect of the substitution was seen regarding the binding of interaction partners, intracellular localization, or stability of the protein. Although the precise mechanism for inflammasome activation remains to be determined, we hypothesize that the ensuing chronic inflammation is important for the development of corneal vascularization and keloids seen in OPDKD.

Acknowledgements

We would like to thank Unni Larsen (Department of Ophthalmology, Haukeland University Hospital, Bergen, Norway) for technical assistance. The immunofluorescence imaging was performed at the Molecular Imaging Center (MIC), Department of Biomedicine, University of Bergen, Norway. The work was supported by grants from the Western Norway Regional Health Authority (911977 and 912161), Inger Holm's Memory Foundation, and Dr. Jon S. Larsen's Foundation.

Author contributions

HA, RCMH, ER, OB, and CB conceived and supervised the study. IC, OB, ER, DJMP, and CB designed experiments. AECM and MT collected clinical specimens. IC, OB, and RM performed the experiments. IC, DJMP, OB, GH, ER, and CB analyzed data. IC,

ER, and CB wrote the manuscript. All authors reviewed and approved the final manuscript.

Data accessibility

All data generated or analyzed during this study are included in this published article and its additional files.

References

- Landsend ES, Utheim ØA, Pedersen HR, Lagali N, Baraas RC and Utheim TP (2018) The genetics of congenital aniridia—a guide for the ophthalmologist. *Surv Ophthalmol* **63**, 105–113.
- Aslan D, Akata RF, Holme H, Vulliamy T and Dokal I (2012) Limbal stem cell deficiency in patients with inherited stem cell disorder of dyskeratosis congenita. *Int Ophthalmol* **32**, 615–622.
- Xu L, Jensen H, Johnston JJ, Di Maria E, Kloth K, Cristea I, Sapp JC, Darling TN, Huryn LA, Tranebjærg L *et al.* (2018) Recurrent, activating variants in the receptor tyrosine kinase DDR2 cause Warburg-Cinotti syndrome. *Am J Hum Genet* **103**, 976–983.
- Bredrup C, Cristea I, Safieh LA, Di Maria E, Gjertsen BT, Tveit KS, Thu F, Bull N, Edward DP, Hennekam RCM *et al.* (2021) Temperature-dependent autoactivation associated with clinical variability of PDGFRB Asn666 substitutions. *Hum Mol Genet* **30**, 72–77.
- Islam SI and Wagoner MD (2001) Pterygium in young members of one family. *Cornea* **20**, 708–710.
- Abarca H, Mellgren AE, Trubnykova M, Haugen OH, Hovding G, Tveit KS, Houge G, Bredrup C and Hennekam RC (2014) Ocular pterygium—digital keloid dysplasia. *Am J Med Genet A* **164A**, 2901–2907.
- Haugen OH and Bertelsen T (1998) A new hereditary conjunctivo-corneal dystrophy associated with dermal keloid formation. Report of a family. *Acta Ophthalmol Scand* **76**, 461–465.
- McKenna A, Hanna M, Banks E, Sivachenko A, Cibulskis K, Kernytzky A, Garimella K, Altshuler D, Gabriel S, Daly M *et al.* (2010) The genome analysis toolkit: a MapReduce framework for analyzing next-generation DNA sequencing data. *Genome Res* **20**, 1297–1303.
- Van der Auwera GA, Carneiro MO, Hartl C, Poplin R, Del Angel G, Levy-Moonshine A, Jordan T, Shakir K, Roazen D, Thibault J *et al.* (2013) From FastQ data to high confidence variant calls: the genome analysis toolkit best practices pipeline. *Curr Protoc Bioinformatics* **43**, 11.0.1–11.0.33.
- Danecek P, Auton A, Abecasis G, Albers CA, Banks E, DePristo MA, Handsaker RE, Lunter G, Marth GT, Sherry ST *et al.* (2011) The variant call format and VCFtools. *Bioinformatics* **27**, 2156–2158.
- Wang K, Li M and Hakonarson H (2010) ANNOVAR: functional annotation of genetic variants from high-throughput sequencing data. *Nucleic Acids Res* **38**, e164.
- Cristea I, Bruland O, Rødahl E and Bredrup C (2021) K+ regulates relocation of Pellino-2 to the site of NLRP3 inflammasome activation in macrophages. *FEBS Lett* **595**, 2437–2446.
- Pear WS, Nolan GP, Scott ML and Baltimore D (1993) Production of high-titer helper-free retroviruses by transient transfection. *Proc Natl Acad Sci USA* **90**, 8392–8396.
- Swift S, Lorens J, Achacoso P and Nolan GP (2001) Rapid production of retroviruses for efficient gene delivery to mammalian cells using 293T cell-based systems. *Curr Protoc Immunol* **Chapter 10**, Unit 10.7C.
- Bredrup C, Stokowy T, McGaughran J, Lee S, Sapkota D, Cristea I, Xu L, Tveit KS, Hovding G, Steen VM *et al.* (2018) A tyrosine kinase-activating variant Asn666Ser in PDGFRB causes a progeria-like condition in the severe end of Penttinen syndrome. *Eur J Hum Genet* **27**, 574–581.
- Cristea I, Bruland O, Aukrust I, Rødahl E and Bredrup C (2021) Pellino-2 in nonimmune cells: novel interaction partners and intracellular localization. *FEBS Lett* **595**, 2909–2921.
- Jensen LE and Whitehead AS (2003) Pellino2 activates the mitogen activated protein kinase pathway. *FEBS Lett* **545**, 199–202.
- Kim TW, Yu M, Zhou H, Cui W, Wang J, DiCorleto P, Fox P, Xiao H and Li X (2012) Pellino 2 is critical for toll-like receptor/interleukin-1 receptor (TLR/IL-1R)-mediated post-transcriptional control. *J Biol Chem* **287**, 25686–25695.
- Wade EM, Daniel PB, Jenkins ZA, McInerney-Leo A, Leo P, Morgan T, Addor MC, Adès LC, Bertola D, Bohring A *et al.* (2016) Mutations in MAP3K7 that Alter the activity of the TAK1 signaling complex cause Frontometaphyseal dysplasia. *Am J Hum Genet* **99**, 392–406.
- Humphries F, Bergin R, Jackson R, Delagic N, Wang B, Yang S, Dubois AV, Ingram RJ and Moynagh PN (2018) The E3 ubiquitin ligase Pellino2 mediates priming of the NLRP3 inflammasome. *Nat Commun* **9**, 1560.
- Jin H, Peng X, He Y, Ruganzu JB and Yang W (2020) Tanshinone IIA suppresses lipopolysaccharide-induced neuroinflammatory responses through NF- κ B/MAPKs signaling pathways in human U87 astrocytoma cells. *Brain Res Bull* **164**, 136–145.
- Strelow A, Kollwe C and Wesche H (2003) Characterization of Pellino2, a substrate of IRAK1 and IRAK4. *FEBS Lett* **547**, 157–161.

- 23 Kawan S, Backlund MP, Immonen AT, Kivelä TT and Turunen JA (2022) Functional consequences of pathogenic variant c.61G>C in the inflammasome gene NLRP3 underlying keratitis fugax hereditaria. *Br J Ophthalmol* doi: [10.1136/bjo-2022-321825](https://doi.org/10.1136/bjo-2022-321825)
- 24 Sun N and Zhang H (2018) Pyroptosis in pterygium pathogenesis. *BioSci Rep* **38**, BSR20180282.
- 25 Xu J, Chen P, Luan X, Yuan X, Wei S, Li Y, Guo C, Wu X and Di G (2022) The NLRP3 activation in infiltrating macrophages contributes to corneal fibrosis by inducing TGF- β 1 expression in the corneal epithelium. *Invest Ophthalmol Vis Sci* **63**, 15.
- 26 Dong M, Yang L, Qu M, Hu X, Duan H, Zhang X, Shi W and Zhou Q (2018) Autocrine IL-1 β mediates the promotion of corneal neovascularization by senescent fibroblasts. *Am J Physiol Cell Physiol* **315**, C734–C743.
- 27 Lee S, Kim SK, Park H, Lee YJ, Park SH, Lee KJ, Lee DG, Kang H and Kim JE (2020) Contribution of autophagy-Notch1-mediated NLRP3 Inflammasome activation to chronic inflammation and fibrosis in keloid fibroblasts. *Int J Mol Sci* **21**, 8050.
- 28 Vinaik R, Barayan D, Auger C, Abdullahi A and Jeschke MG (2020) Regulation of glycolysis and the Warburg effect in wound healing. *JCI. Insight* **5**, e138949.
- 29 Wang YC, Zhao FK, Liu Q, Yu ZY, Wang J and Zhang JS (2021) Bibliometric analysis and mapping knowledge domain of pterygium: 2000–2019. *Int J Ophthalmol* **14**, 903–914.
- 30 Kate A and Basu S (2022) A review of the diagnosis and treatment of Limbal stem cell deficiency. *Front Med (Lausanne)* **9**, 836009.
- 31 Lin CC, Huoh YS, Schmitz KR, Jensen LE and Ferguson KM (2008) Pellino proteins contain a cryptic FHA domain that mediates interaction with phosphorylated IRAK1. *Structure* **16**, 1806–1816.
- 32 Malireddi RKS, Gurung P, Mavuluri J, Dasari TK, Klco JM, Chi H and Kanneganti TD (2018) TAK1 restricts spontaneous NLRP3 activation and cell death to control myeloid proliferation. *J Exp Med* **215**, 1023–1034.
- 33 Schmid-Burgk JL, Chauhan D, Schmidt T, Ebert TS, Reinhardt J, Endl E and Hornung V (2016) A genome-wide CRISPR (clustered regularly interspaced short palindromic repeats) screen identifies NEK7 as an essential component of NLRP3 inflammasome activation. *J Biol Chem* **291**, 103–109.
- 34 He Y, Zeng MY, Yang D, Motro B and Nunez G (2016) NEK7 is an essential mediator of NLRP3 activation downstream of potassium efflux. *Nature* **530**, 354–357.
- 35 Cho KA and Kang PB (2015) PLIN2 inhibits insulin-induced glucose uptake in myoblasts through the activation of the NLRP3 inflammasome. *Int J Mol Med* **36**, 839–844.
- 36 Mihalas AB and Hevner RF (2017) Control of neuronal development by T-box genes in the brain. *Curr Top Dev Biol* **122**, 279–312.
- 37 Hedtke V and Bakovic M (2019) Choline transport for phospholipid synthesis: an emerging role of choline transporter-like protein 1. *Exp Biol Med (Maywood)* **244**, 655–662.

Supporting information

Additional supporting information may be found online in the Supporting Information section at the end of the article.

Fig. S1. Difference in protein binding to the magnetic HA beads depending on the wash buffer used following co-immunoprecipitation.

Table S1. Results of prediction software for the novel variants.

Table S2. Cloning primers.

Table S3. Components of the lysis buffer and washing buffer used for co-immunoprecipitation of target proteins.